

A Short and Nearly Symmetrical Intramolecular Hydrogen Bond: X-ray and Neutron Diffraction Analysis of 2,2'-(1,3-Diaminopropane)bis(2-methyl-3-butanone oximato)nickel(II) Chloride Hydrate

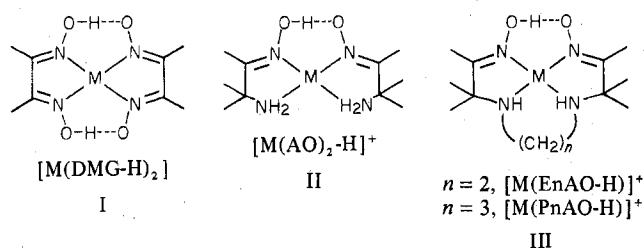
M. SAKHAWAT HUSSAIN and E. O. SCHLEMPER*

Received February 27, 1979

A combined room-temperature neutron and X-ray diffraction study of hydrated 2,2'-(1,3-diaminopropane)bis(2-methyl-3-butanone oximato)nickel(II) chloride, $[\text{Ni}(\text{PnAO-H})]\cdot x\text{H}_2\text{O}$, $[\text{Ni}(\text{C}_{13}\text{H}_{27}\text{N}_4\text{O}_2)]\text{Cl}\cdot x\text{H}_2\text{O}$ ($x = 1$ or 1.5), has been performed to investigate the influence of steric requirements of the ligand and the size of the metal ion on the short intramolecular $\text{O}\cdots\text{O}$ hydrogen bond. $[\text{Ni}(\text{PnAO-H})]\text{Cl}\cdot x\text{H}_2\text{O}$ crystallizes with four molecules in an orthorhombic unit cell of symmetry $P2_12_12_1$ with $a = 10.997$ (4) Å, $b = 12.683$ (5) Å, and $c = 13.369$ (4) Å for the monohydrated complex. Three-dimensional Patterson and Fourier methods followed by full-matrix least-squares refinement gave $R(F^2) = 0.081$ with 1637 neutron data and $R(F^2) = 0.064$ with 2501 X-ray data. The complex cation has square-planar coordination about the nickel atom. The water molecule and chloride ion are extensively hydrogen bonded to each other and to the amine hydrogen atoms of the cation. The hydrogen atom in the intramolecular hydrogen bond is nearly symmetrically disposed in the $\text{O}-\text{H}\cdots\text{O}$ bond with a short (2.409 (10) Å) $\text{O}\cdots\text{O}$ distance. The $\text{O}-\text{H}$ bond lengths for the hydrogen bond are 1.16 (2) and 1.26 (2) Å and the $\text{O}-\text{H}-\text{O}$ angle is 170 (1)°. The potential for the intramolecular hydrogen bond apparently has a broad and nearly symmetrical single minimum. The methyl groups attached to sp^2 carbon atoms have large rotational amplitudes resulting in short apparent $\text{C}-\text{H}$ bond lengths (1.04 (3) Å average). Other average uncorrected bond distances involving hydrogen atoms are $\text{O}-\text{H}$ (in H_2O) = 0.92 (4) Å, $\text{N}-\text{H}$ = 1.04 (1) Å, and $\text{C}-\text{H}$ = 1.08 (3) Å for methyl groups attached to sp^3 carbon atoms. A comparison with the reported work on the α -amine oxime (AO) complexes has shown that the earlier conclusion about the resemblance of steric requirements of PnAO and two coordinated AO's is maintained. The $\text{Ni}-\text{N}$ (amine) and $\text{Ni}-\text{N}$ (oxime) distances in the present complex are 0.04–0.05 Å longer than the corresponding distances in $\text{Ni}(\text{II})-\text{AO}$ and $-\text{EnAO}$ complexes, whereas the $\text{O}\cdots\text{O}$ distance is about 0.06 Å shorter than that observed in the $\text{EnAO}-\text{Ni}(\text{II})$ complex. The predicted thermodynamic stability based upon bond distances is in good agreement with the observed thermodynamic and spectral data on nickel(II)- α -amine oxime complexes.

Introduction

Several metal complexes (I–III) of the dimethylglyoxime



(DMG)¹ and α -amine oximes AO, EnAO, and PnAO have been studied by neutron^{2–4} and X-ray⁵ diffraction to obtain information regarding the role of the size of metal ions and the steric requirements of the ligands on the short intramolecular $\text{O}\cdots\text{O}$ hydrogen bond and associated potential functions. The completed studies have revealed that (1) the $\text{O}\cdots\text{O}$ bond length, in the complexes of the same ligand or of sterically similar ligands, varies by changing the size of the central metal atom, (2) an ethylene bridge across the hydrogen bond increases the $\text{O}\cdots\text{O}$ distance, relative to the unbridged compound, while a propylene bridge has no significant effect on this distance for first series transition metals, and (3) the asymmetry of the hydrogen bond is related to the $\text{O}\cdots\text{O}$ distance, i.e., the larger the distance the more asymmetrical is the bond.

With three exceptions,^{2–4} the structural analyses were done by X-ray diffraction without precise location of the hydrogen atoms. Prior to this investigation, none of the PnAO complexes have been studied by neutron diffraction.

Experimental Section

Synthesis and Crystal Preparation. The compound was prepared by dissolving solid $\text{NiCl}_2\cdot 6\text{H}_2\text{O}$ (Baker Chemical) in a 1:1 HCl solution with 5% more than the stoichiometric amount of PnAO.⁶ The pH of the solution was raised to 7 with 5 M NaOH and the resulting clear solution was allowed to evaporate at room temperature over a period of 3–4 days until most of the sodium chloride crystallized out and was separated twice from the clear yellow solution of the complex.

Table I. Crystal Data for the $[\text{Ni}(\text{PnAO-H})]\text{Cl}\cdot x\text{H}_2\text{O}$

	neutron data	X-ray data
space group:	$P2_12_12_1$	$Z = 4$
density, obsd:	1.34 g cm^{-3}	
formula	$\text{Ni}(\text{C}_{13}\text{H}_{27}\text{N}_4\text{O}_2)\text{Cl}\cdot \text{H}_2\text{O}$	$\text{Ni}(\text{C}_{13}\text{H}_{27}\text{N}_4\text{O}_2)\text{Cl}\cdot 1.5\text{H}_2\text{O}$
formula wt	383.4	392.4
calcd density, g cm^{-3}	1.366	1.394
bounding faces	(110), ($\bar{1}\bar{1}0$), ($\bar{1}10$), ($1\bar{1}0$), ($\bar{1}01$), (101)	(110), ($\bar{1}\bar{1}0$), ($\bar{1}10$), ($1\bar{1}0$), ($00\bar{1}$), (011), ($0\bar{1}1$), ($\bar{1}11$)
radiation, λ (Å)	Mo $K\alpha$, 0.7107	Mo $K\alpha$, 0.7107
a , Å	10.997 (4)	11.010 (3)
b , Å	12.683 (5)	12.664 (4)
c , Å	13.369 (4)	13.417 (4)
V , Å ³	1864.7	1870.6

On further evaporation large rectangular crystals of the complex were formed along with some small crystals of the complex and of sodium chloride. The presence of a small amount of sodium chloride in the concentrated solution of the complex facilitated the growth of larger crystals since efforts to obtain such crystals by evaporating a concentrated solution of pure crystals of the complex were not successful. The presence of the PnAO moiety in the complex was confirmed by its infrared spectrum.

Unit Cell and Space Group. The lattice parameters for $[\text{Ni}(\text{C}_{13}\text{H}_{27}\text{N}_4\text{O}_2)]\text{Cl}\cdot x\text{H}_2\text{O}$ were determined with a Picker diffractometer from a least-squares refinement of the setting angles of 15 reflections. The cell parameters used for neutron data were accurately determined on the X-ray diffractometer by using a small piece ($0.29 \times 0.33 \times 0.34$ mm) from the second neutron crystal and carefully centering 15 reflections. These cell constants were used in all calculations with the neutron data (Table I).

Precession photographs and the collected data sets revealed the systematic absences $h00$ for $h = 2n + 1$, $0k0$ for $k = 2n + 1$, and $00l$ for $l = 2n + 1$, consistent with the space group $P2_12_12_1$.

X-ray Data Collection and Structure Analysis. hkl and $\bar{h}\bar{k}l$ X-ray data were collected on a Picker diffractometer by using conditions given in Table II. Correction was made for a 12% decrease in the intensities of the standard reflections observed during the data collection. After correction⁹ for background, Lorentz-polarization,

Table II. Neutron and X-ray Intensity Data Collection

	neutron		X-ray
	crystal A	crystal B	
cryst dimens, mm	3.2 × 1.5 × 2.1	3.0 × 1.7 × 1.8	0.13 × 0.14 × 0.22
scan speed or step size	0.08°/step	0.08°/step	1°/min
total no. of steps	31	31	
scan range (2θ), deg	2.48	2.48	Kα ₁ - 0.50 to Kα ₂ + 0.50
2θ limit, deg	85	95	55
octant measd	<i>hkl</i>	<i>hkl, hkl</i>	<i>hkl, hkl</i>
total reflectns measd	831	1900	3659
stand reflectns	(910), (060), (4,11,0)	(910), (060), (4,11,0)	(023), (052), (040)
interval, std reflectns measd	75	75	~80
intensity loss in std reflectns, %	11	7	12
abs coef (μ), cm ⁻¹	2.296	2.296	11.87
transmission factor for abs cor		0.62 to 0.75	0.86 to 0.90
no. of unique data		1730	3154
agreement factor on averaging		0.041	0.041
data used in calcs		1637 with $I > 1.5\sigma(I)$	2501 with $I > 2\sigma(I)$
no. of variables refined		461	209
goodness of fit, <i>S</i>		1.464	1.450
final discrepancy indices			
$R(F^2)$		0.081	0.064
$R_w(F^2)$		0.107	0.115

and absorption effects, 3659 data were averaged to 3154 reflections, of which 2501 had $I > 2\sigma(I)$. While averaging the data, we took into account the nonequivalence of Friedel pairs.

Neutral atomic scattering factors of Cromer and Waber^{8b} were used for all atoms except hydrogen, for which the values of Stewart, Davidson, and Simpson^{8a} were taken. The values of real and imaginary components of anomalous dispersion corrections for the nickel and chlorine atoms were obtained from Cromer^{8c} and were included in calculated structure factors.^{8d}

Efforts to solve the structure by MULTAN were unsuccessful. A Patterson map revealed the position of the nickel atom and successive Fourier syntheses established the coordinates of all nonhydrogen atoms in the complex and the oxygen atom of a water of hydration. After a few cycles of least-squares refinement, idealized positions for all the hydrogen atoms were calculated, consistent with difference Fourier syntheses, and refinement with anisotropic temperature factors for all nonhydrogen atoms and fixed atom contributions for the hydrogen atoms led to discrepancy indices¹⁰ of $R(F_o^2) = 0.101$ and $R_w(F_o^2) = 0.161$. A difference Fourier map at this stage revealed the coordinates of the oxygen atom of another water molecule.

Since $P2_12_12_1$ is a noncentrosymmetric space group, there are two enantiomers possible. For determination of the absolute configuration in the crystal selected for the present study, the signs of *h*, *k*, and *l* were reversed.¹¹ Refining the same parameters using the alternate data set led to higher values for discrepancy indices ($R(F_o^2)$ values of 0.085 vs. 0.072 using the same number of variables), suggesting that the original model was preferred and that model was chosen for subsequent refinement. The final least-squares refinement of 209 variables, including an occupancy factor for the oxygen atom of the second water of hydration, converged to $R(F_o^2) = 0.064$ and $R_w(F_o^2) = 0.115$. The oxygen atom of the second water molecule had an occupancy factor of 0.5. A difference Fourier map had all residual peaks less than 0.060 e Å⁻³. After the final cycle the shifts on all refined parameters were below one-tenth of their standard deviation.

Neutron Data Collection and Structure Analysis. The neutron intensity data were collected on a locally automated Mitsubishi four-circle diffractometer at the University of Missouri Research Reactor. The neutron beam was monochromated by a Be crystal. The neutron wavelength, 1.116 Å, used during the data collection on the first crystal was determined by using the reported cell dimensions for NaOAc·3H₂O,⁷ and the wavelength of 1.0685 Å used for the second crystal was obtained by using a Si ($a = 5.4308$ Å) crystal. Two data sets were collected by using a θ - 2θ step-scan procedure and conditions given in Table II. The lattice constants used for neutron data collection were obtained by least-squares fits of the orientation angles of 21 automatically centered reflections. Data collection on the crystal A beyond $2\theta = 85^\circ$ was terminated due to a decrease in the intensities of the standard reflections accompanied by a slight shattering and opaqueness of the crystal. Only the initial 825 reflections having less than 11% decrease in the intensities of the standard reflections were included in averaging of the data from crystal A. The intensities of

the standards for crystal B showed no variations greater than 7% during the 3 weeks required for data collection. The data were corrected⁹ for decay, Lorentz, and absorption effects, and the data of the two crystals were merged to yield 1730 independent reflections. The 1637 having $I > 1.5\sigma(I)$ were used in the refinement. The variances of F_o^2 were calculated from $\sigma^2(F_o^2) = \sigma_c^2(F_o^2) + (0.05F_o^2)^2$ where $\sigma_c^2(F_o^2)$ is determined from the counting statistics and 0.05 is an empirical "ignorance factor".

The atomic scattering cross sections^{8c} used in the neutron analysis were $b_{Ni} = 1.02$, $b_{Cl} = 0.958$, $b_N = 0.94$, $b_O = 0.575$, and $b_H = -0.372$ (all in units 10⁻¹² cm). The X-ray parameters for the nonhydrogen atoms (without the half occupancy water oxygen) were used as starting coordinates. A full-matrix least-squares refinement of the positional and isotropic temperature parameters for all nonhydrogen atoms gave $R(F^2) = 0.413$ and $R_w(F^2) = 0.512$. The coordinates for hydrogen atoms located from a difference Fourier synthesis were first refined isotropically by three cycles of least-squares refinement, and finally three more cycles of anisotropic refinement with 461 parameters, including a secondary extinction correction ($g = 3.0986 \times 10^{-5}$), using 1637 reflections led to $R(F^2) = 0.081$ and $R_w(F^2) = 0.107$. A difference Fourier map at this stage revealed no significant negative nuclear scattering density nor any positive nuclear scattering density corresponding to the oxygen atom of the half-occupancy water molecule. Inclusion of the half-occupancy oxygen atom at the position obtained from X-ray analysis and refining its occupancy factor revealed less than one-tenth occupancy and no improvement in agreement factors, suggesting absence of the partial water of hydration in the crystal used for neutron data. The shifts in parameters after a few more refinement cycles were less than one-hundredth of their standard deviations.

Results and Discussion

General Description of the Crystal and Molecular Structure.

The final positional and thermal parameters from the X-ray and neutron diffraction analyses are given in Tables III-VII. Tables V-VII are deposited as supplementary material.¹² The intermolecular distances and bond angles involving nonhydrogen atoms are compared in Figures 1 and 2. Some significant intermolecular contact distances and distances involving hydrogen atoms are given in Table VIII. Structure factor tables for both data sets are available.¹² Least-squares planes of interest calculated from neutron-determined coordinates are provided in Table IX.

The crystal structure of [Ni(PnAO-H)]Cl·H₂O, using neutron diffraction parameters, is depicted stereoscopically in Figure 3. The crystal used for the X-ray data has a half-occupancy oxygen of a second water molecule at 2.99 (2) Å from the Cl⁻ ion in addition to one water molecule of hydration present in both crystals. The *c*-axis length of 13.417 (4) Å

Table III. Positional Parameters for Nonhydrogen Atoms

atom	neutron diffraction			X-ray diffraction		
	x	y	z	x	y	z
Ni	0.1348 (3)	-0.0077 (2)	0.1816 (2)	0.1349 (1)	-0.0076 (1)	0.1817 (1)
Cl	0.3674 (5)	0.2259 (5)	0.0939 (4)	0.3674 (2)	0.2256 (2)	0.0939 (2)
O(1)	0.0204 (6)	-0.1241 (5)	0.0257 (4)	0.0201 (4)	-0.1240 (4)	0.0265 (3)
O(2)	0.2192 (7)	-0.1861 (5)	0.0730 (5)	0.2208 (4)	-0.1860 (4)	0.0718 (3)
O(3)	0.0836 (14)	0.2702 (10)	0.0739 (9)	0.0800 (5)	0.2703 (4)	0.0744 (4)
N(1)	0.2740 (3)	0.0469 (3)	0.2534 (3)	0.2725 (4)	0.0462 (4)	0.2530 (4)
N(2)	0.2449 (3)	-0.1140 (3)	0.1430 (2)	0.2446 (5)	-0.1137 (4)	0.1443 (4)
N(3)	0.0064 (3)	-0.0529 (3)	0.0986 (2)	0.0064 (4)	-0.0522 (4)	0.1000 (3)
N(4)	0.0213 (3)	0.1038 (3)	0.2150 (3)	0.0224 (4)	0.1045 (4)	0.2144 (4)
C(1)	0.3678 (4)	-0.0388 (4)	0.2703 (4)	0.3674 (5)	-0.0397 (4)	0.2696 (4)
C(2)	0.3503 (4)	-0.1168 (4)	0.1863 (4)	0.3482 (5)	-0.1164 (4)	0.1861 (5)
C(3)	-0.0988 (4)	-0.0069 (4)	0.1078 (3)	-0.0977 (5)	-0.0077 (5)	0.1087 (4)
C(4)	-0.1077 (4)	0.0667 (4)	0.1960 (4)	-0.1061 (5)	0.0675 (5)	0.1955 (5)
C(5)	-0.2022 (6)	-0.0287 (7)	0.0397 (6)	-0.2024 (6)	-0.0303 (6)	0.0405 (6)
C(6)	-0.1907 (6)	0.1606 (6)	0.1734 (7)	-0.1899 (6)	0.1613 (6)	0.1738 (6)
C(7)	-0.1555 (7)	0.0036 (7)	0.2855 (5)	-0.1546 (6)	0.0037 (7)	0.2837 (5)
C(8)	0.4445 (7)	-0.1971 (6)	0.1589 (6)	0.4443 (7)	-0.1964 (6)	0.1600 (6)
C(9)	0.4958 (6)	0.0075 (7)	0.2689 (7)	0.4950 (6)	0.0095 (6)	0.2682 (6)
C(10)	0.3474 (7)	-0.0963 (5)	0.3697 (5)	0.3465 (6)	-0.0972 (5)	0.3692 (5)
C(11)	0.0367 (6)	0.1627 (6)	0.3103 (5)	0.0380 (6)	0.1628 (5)	0.3104 (5)
C(12)	0.1662 (6)	0.2026 (5)	0.3238 (5)	0.1650 (6)	0.2029 (5)	0.3216 (5)
C(13)	0.2558 (6)	0.1142 (5)	0.3425 (4)	0.2556 (6)	0.1143 (5)	0.3433 (5)
O4				0.4661 (15)	0.0323 (14)	-0.0057 (13)

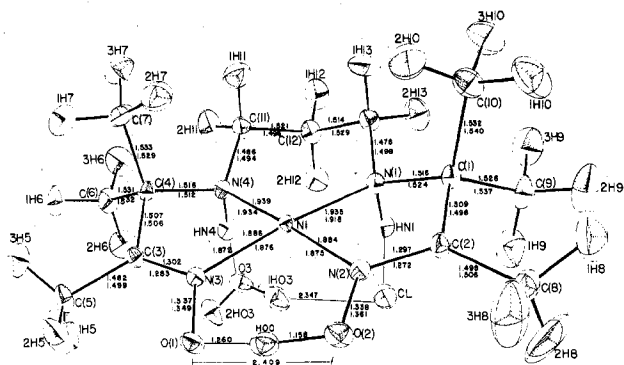


Figure 1. Bond distances and numbering system in $[\text{Ni}(\text{PnAO-H})]\text{Cl}\cdot\text{H}_2\text{O}$. In numbering hydrogen atoms the last number in the label corresponds to the carbon atom to which that hydrogen is attached. The neutron results are given on the first line and the X-ray results on the second. The standard deviations in the distances are Ni-N = 0.004–0.006, N-C = 0.006–0.008, C-C = 0.007–0.009, N-O = 0.006–0.007, and N-H = 0.01. (Å units are used for the neutron study.)

for the crystal with 1.5 water molecules is significantly longer than the corresponding axis length of 13.369 (4) Å for the monohydrate crystal.

The ligand puckering is very similar to that observed in the $[\text{Pd}(\text{PnAO-H})]\text{NO}_3$ complex.⁵ The four nitrogens surrounding the nickel atom define a weighted least-squares plane (plane II, Table IX) with the nickel atom slightly out of the plane and with a slight tetrahedral puckering of the nitrogen atoms. The six-membered chelate ring with a propylene bridge is in the chair configuration with the Ni atom 1.426 Å below and C(12) atom 1.999 Å above the plane defined by N(1), N(4), C(11), and C(13) (plane IV, Table IX). The two five-membered chelate rings are puckered (planes V, VI) to accommodate the strain introduced by a short N-C(sp²) bond as compared to almost equal C(sp²)-C(sp³) and N-C(sp³) bonds in these rings. Large portions of the complex cation are related by mirror symmetry across a plane passing approximately through the C(12), Ni, and HOO atoms.

There is extensive hydrogen bonding involving the waters of hydration, the Cl⁻ ion, and amine hydrogen atoms. The closest intermolecular contacts are given in Table VIII. The hydrogen-bond angles and donor atom-acceptor atom dis-

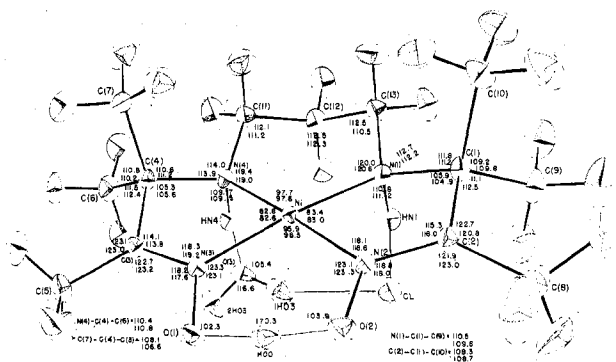


Figure 2. Bond angles in $[\text{Ni}(\text{PnAO-H})]\text{Cl}\cdot\text{H}_2\text{O}$. The neutron diffraction results are on the first line, followed by the X-ray results on the second. The standard deviations in the angles are N-Ni-N = 0.2, C-N-Ni = 0.3–0.4, N-C-C = 0.4–0.5, C-C-C = 0.5–0.6, O-N-Ni = 0.4, and O-N-C = 0.4–0.6. (Degrees are used for the neutron study.)

tances are normal. Each hydrogen atom of the water molecule is involved in a weak hydrogen bond 2.35 Å from the chloride ion. Both amine hydrogens are engaged in hydrogen bonding with a HN1-Cl distance of 2.262 Å and an O(3)-HN4 distance of 1.886 Å. The hydrogen bonding involving one amine nitrogen (N4) is stronger than that with the other amine nitrogen (N1). Similar unequal hydrogen bonding distances were observed in $[\text{Ni}(\text{AO})_2\text{-H}]^+$ complex.⁵ The X-H...Y angles are all close to linear (average angle = 166°). None of the oxime oxygen atoms are involved in intermolecular hydrogen bonding. The closest hydrogen atom (3H8) to O(2) is at 2.384 Å and hydrogen atom 2H5 is at a distance of 2.352 Å from O(1). The crystal structure is thus stabilized by an extensive network of hydrogen bonds. The oxygen of the half-occupancy water molecule in the X-ray crystal is at 2.993 Å from the Cl⁻ ion.

The observed differences between the neutron and the X-ray results for the nonhydrogen atoms are not significant when compared with the standard deviations.

Bond Distances and Bond Angles. The overall distances and angles are in good agreement with those observed in other similar complexes. Unlike the case for the Ni(II)- and Pt(II)-AO complexes^{2,3} or the $[\text{Ni}(\text{EnAO-H})]^+$ complex,⁴ no significant differences were observed in chemically equivalent

Table IV. Positional Parameters for Hydrogen Atoms

atom	neutron diffraction			X-ray diffraction		
	x	y	z	x	y	z
HN1	0.3111 (9)	0.0953 (8)	0.1993 (8)	0.3254	0.0821	0.2347
HN4	0.0400 (10)	0.1598 (8)	0.1596 (9)	0.0175	0.1619	0.1612
1H5	-0.2125 (22)	0.0350 (20)	-0.0120 (18)	-0.1923	0.0254	0.0071
2H5	-0.1892 (15)	-0.0975 (15)	0.0013 (14)	-0.1934	-0.0799	0.0082
3H5	-0.2828 (13)	-0.0294 (25)	0.0797 (15)	-0.2785	-0.0279	0.0760
1H6	-0.2832 (12)	0.1345 (12)	0.1612 (13)	-0.2724	0.1294	0.1570
2H6	-0.1596 (16)	0.2039 (12)	0.1093 (14)	-0.1618	0.2089	0.1321
3H6	-0.1908 (15)	0.2177 (13)	0.2365 (14)	-0.1983	0.2067	0.2352
1H7	-0.0930 (14)	-0.0563 (13)	0.3087 (11)	-0.1292	-0.0489	0.3223
2H7	-0.2371 (15)	-0.0358 (14)	0.2648 (12)	-0.2402	-0.0238	0.2686
3H7	-0.1778 (13)	0.0559 (16)	0.3481 (12)	-0.1714	0.0567	0.3343
1H8	0.4989 (19)	-0.2180 (18)	0.2184 (17)	0.5060	-0.2040	0.2060
2H8	0.4998 (26)	-0.1702 (25)	0.1053 (24)	0.4809	-0.1790	0.0987
3H8	0.4022 (19)	-0.2665 (17)	0.1307 (24)	0.4072	-0.2645	0.1545
1H9	0.5150 (14)	0.0496 (17)	0.1977 (17)	0.5281	0.0424	0.2126
2H9	0.5607 (12)	-0.0482 (13)	0.2802 (16)	0.5506	-0.0409	0.2887
3H9	0.5104 (13)	0.0640 (12)	0.3324 (14)	0.4934	0.0664	0.3174
1H10	0.4039 (17)	-0.1663 (13)	0.3708 (11)	0.3690	-0.1940	0.3740
2H10	0.2534 (16)	-0.1176 (12)	0.3786 (11)	0.2648	-0.0877	0.3866
3H10	0.3713 (15)	-0.0495 (12)	0.4306 (10)	0.3971	-0.0639	0.4180
1H11	0.0147 (15)	0.1088 (16)	0.3734 (11)	0.0209	0.1161	0.3662
2H11	-0.0266 (15)	0.2261 (14)	0.3119 (14)	-0.0197	0.2204	0.3163
1H12	0.1687 (15)	0.2551 (12)	0.3882 (13)	0.1664	0.2558	0.3750
2H12	0.1937 (15)	0.2492 (10)	0.2593 (12)	0.1856	0.2399	0.2618
1H13	0.2225 (15)	0.0670 (10)	0.4035 (8)	0.2228	0.0702	0.3958
2H13	0.3416 (14)	0.1472 (12)	0.3646 (12)	0.3301	0.1421	0.3652
HOO	0.1233 (11)	-0.1624 (9)	0.0453 (8)	0.0851	-0.1600	0.0175
1HO3	0.1618 (23)	0.2591 (19)	0.0589 (16)	0.1618	0.2591	0.0589
2HO3	0.0347 (17)	0.2714 (13)	0.0163 (15)	0.0347	0.2714	0.0163

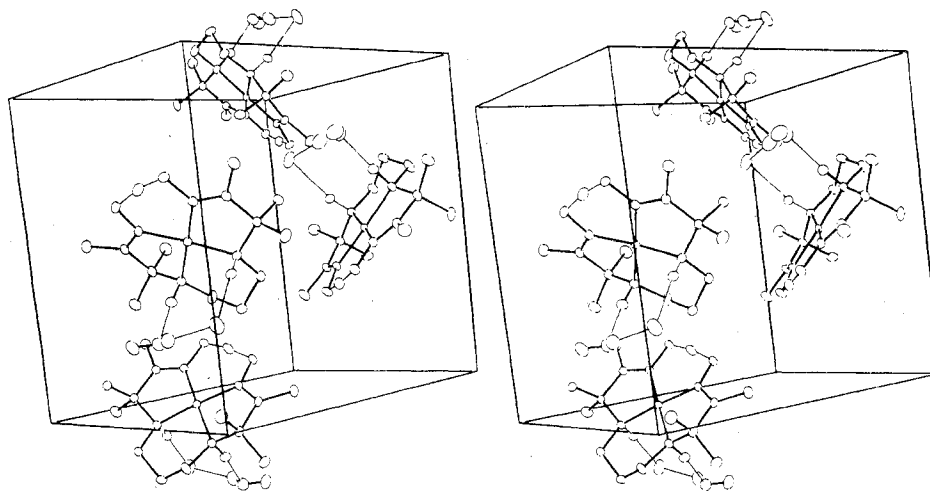


Figure 3. Stereoscopic view showing packing of the molecules in the acentric orthorhombic unit cell. The crystallographic *a* axis lies along the horizontal direction, the *c* axis is in the vertical direction, and the *b* axis completes the right-handed coordinate system.

bond distances; e.g., pairs of Ni–N(oxime), Ni–N(amine), N–O, N(oxime)–C(sp²), and N(amine)–C(sp³) distances are all equal within one standard deviation. Similar to previously studied amine oxime complexes (Table X), the metal–N(amine) distances are about 0.05 Å larger than the metal–N(oxime) distances. Furthermore, these distances are significantly longer than the corresponding distances in the Ni–AO² and Ni–EnAO⁴ complexes. The average Ni–N(amine) distance 1.937 Å in the present study is significantly longer than that of 1.877 or 1.908 Å in [Ni(EnAO–H)]⁺ or [Ni(AO)₂–H]⁺, respectively. Similarly, the average Ni–N(oxime) distance 1.884 Å is longer than the corresponding distance in Ni(II) complexes of AO and EnAO. The lengthening of about 0.04–0.05 Å in Ni–N distances is probably indicative of weaker metal–ligand interaction in the PnAO complex compared with the EnAO or AO complexes. The shortest metal–nitrogen distances are exhibited by EnAO, suggesting that this ligand forms the strongest complex with

nickel(II) among these three amine oximes. This might be expected on the basis of chelate effects exerted by three five-membered chelate rings in the EnAO complex as compared with a combination of two five-membered and one six-membered chelate rings in the PnAO complex and only two five-membered rings in the AO complex. The average C–C and C–N distances in the ligand moiety are quite normal and are similar to the corresponding distances in other α-amine oxime complexes.

On the basis of Ni–N bond lengths the relative ligand field strength of α-amine oximes for complex formation would be EnAO > AO > PnAO. The absorption spectra of [Ni(EnAO–H)]⁺, [Ni(AO)–H]⁺, and [Ni(PnAO–H)]⁺ species show¹³ absorption maxima at 382, 412, and 423 mμ, respectively, in the visible region beside two other bands in the ultraviolet. This suggests about a 2370-cm⁻¹ shift toward higher energy in the d–d transition, for the [Ni(EnAO–H)]⁺ complex as compared with the [Ni(PnAO–H)]⁺ complex. The

Table VIII. Neutron-Determined Interatomic Distances (Å) and Angles (deg) Involving Hydrogen Atoms and Intermolecular Hydrogen Bond Parameters

Interatomic Distances and Angles			
O(3)-1HO3	0.89 (4)	C(8)-3H8	1.06 (3)
O(3)-2HO3	0.94 (3)	C(9)-1H9	1.11 (3)
O(3)-HN4	1.87 (2)	C(9)-2H9	1.02 (3)
N(1)-HN1	1.032 (12)	C(9)-3H9	1.12 (2)
N(4)-HN4	1.047 (13)	C(10)-1H10	1.08 (2)
C(5)-1H5	1.07 (3)	C(10)-2H10	1.08 (2)
C(5)-2H5	1.02 (2)	C(10)-3H10	1.04 (2)
C(5)-3H5	1.04 (2)	C(11)-1H11	1.11 (2)
C(6)-1H6	1.08 (2)	C(11)-2H11	1.07 (2)
C(6)-2H6	1.07 (2)	C(12)-1H12	1.09 (2)
C(6)-3H6	1.11 (2)	C(12)-2H12	1.09 (2)
C(7)-1H7	1.07 (2)	C(13)-1H13	1.08 (2)
C(7)-2H7	1.06 (2)	C(13)-2H13	1.07 (2)
C(7)-3H7	1.10 (2)	O(1)-HOO	1.260 (16)
C(8)-1H8	1.03 (2)	O(2)-HOO	1.158 (16)
C(8)-2H8	1.00 (3)		
2HO3-O(3)-HN4	112 (1)	3H8-C(8)-1H8	108 (2)
1HO3-O(3)-2HO3	112 (2)	1H9-C(9)-2H9	109 (2)
HN4-O(3)-1HO3	105 (1)	2H9-C(9)-3H9	103 (1)
HN1-N(1)-Ni	100.3 (6)	3H9-C(9)-1H9	108 (2)
HN4-N(4)-Ni	101.8 (7)	1H10-C(10)-2H10	110 (2)
1H5-C(5)-2H5	109 (2)	2H10-C(10)-3H10	107 (1)
2H5-C(5)-3H5	112 (2)	3H10-C(10)-1H10	108 (1)
3H5-C(5)-1H5	105 (2)	1H11-C(11)-2H11	108 (2)
1H6-C(6)-2H6	109 (1)	1H12-C(12)-2H12	107 (1)
2H6-C(6)-3H6	106 (1)	1H13-C(13)-2H13	108 (1)
3H6-C(6)-1H6	108 (1)	HN1-N(1)-C(13)	105.9 (6)
1H7-C(7)-2H7	107 (2)	HN1-N(1)-C(1)	105.1 (7)
2H7-C(7)-3H7	107 (1)	HN4-N(4)-C(4)	106.0 (7)
3H7-C(7)-1H7	111 (1)	HN4-N(4)-C(11)	104.1 (7)
1H8-C(8)-2H8	107 (2)	O(1)-HOO-O(2)	170.3 (1)
2H8-C(8)-3H8	107 (2)		
Intermolecular Hydrogen Bond Parameters			
C1-N(1)	3.280 (6)	C1-1HO3	2.347 (26)
C1-O(3)	3.27 (2)	C1-O(4)	2.99 (2) ^a
O(3)-N(4)	2.91 (1)	C1-2HO3	2.357 (19)
C1-HN1	2.262 (12)		
C1-HN1-N(1)	168.5 (8)	HN1-C1-O(3)	85.0 (4)
C1-1HO3-O(3)	156 (2)	1HO3-C1-O(4)	114.1 (4) ^a
O(3)-HN4-N(4)	172.3 (1.1)	1HO3-C1-2HO3 ^b	128.7 (8)
HN1-C1-1HO3	89.5 (6)	HN1-C1-O(4)	79.7 (4)

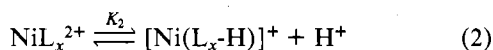
^a X-ray-determined parameters. ^b At position $1/2 + x, 1/2 - y, -z$.

relative energy of the d-d bands indicates the same order for the ligand field strength as predicted on the basis of the metal-nitrogen bond distances. The values¹³ for the thermodynamic stability constant (K_1) for the complex-formation step (eq 1) show strongest complexation for $[\text{Ni}(\text{EnAO-H})]^+$,



$x = 1$ for EnAO and PnAO, $x = 2$ for AO

weakest for $[\text{Ni}(\text{PnAO-H})]^+$, and an intermediate value for the $[\text{Ni}(\text{AO})_2\text{-H}]^+$ complex. Exactly the same relative stability is expected on the basis of the observed Ni-N bond lengths. The thermodynamic constant (K_2) for the hydrogen bond formation (eq 2) has the highest value¹³ for $[\text{Ni}(\text{PnAO-H})]^+$



and lowest for $[\text{Ni}(\text{EnAO-H})]^+$, suggesting a stronger intramolecular hydrogen bond in the former complex as compared with the latter complex. A similar trend in hydrogen bond strength is expected on the basis of the O...O distance; i.e., the shorter the distance the stronger the bond.

The values for the interchelate angles in the present compound (Figure 5) are identical with the corresponding angles in the $[\text{Ni}(\text{AO})_2\text{-H}]^+$ complex and significantly differ from those in the $[\text{Ni}(\text{EnAO-H})]^+$ complex⁴ which is again

Table IX. Equations of Least-Squares Planes and Perpendicular Distances (Å) from These Planes

(A) Plane I through Ni, N(1), N(2), N(3), and N(4)			
$9.035x + 17.924y - 26.740z + 3.648 = 0$			
Ni	-0.130 (7)	N(3)	0.120 (9)
N(1)	0.189 (10)	N(4)	-0.046 (10)
N(2)	-0.008 (8)		
(B) Plane II through N(1), N(2), N(3), and N(4)			
$9.035x + 17.971y - 26.851z + 3.606 = 0$			
N(1)	0.120 (10)	N(2)	-0.069 (8)
N(3)	0.066 (9)	N(4)	-0.109 (10)
Ni	0.191		
(C) Plane III through Ni, O(1), O(2), N(2), N(3), and HOO			
$9.042x + 17.956y - 21.586z + 2.893 = 0$			
Ni	0.052 (6)	N(2)	-0.026 (8)
O(1)	0.294 (16)	N(3)	-0.128 (8)
O(2)	-0.044 (16)	HOO	0.113 (24)
(D) Plane IV through N(1), N(4), C(11), and C(13)			
$9.062x + 27.662y - 18.847z + 0.991 = 0$			
N(1)	-0.005 (10)	C(11)	-0.022 (23)
N(4)	0.004 (10)	C(13)	0.013 (17)
C(12)	1.999	Ni	-1.426
(E) Plane V through Ni, N(1), N(2), C(1), and C(2)			
$9.037x + 13.995y - 20.615z + 2.459 = 0$			
Ni	-0.175 (6)	C(1)	-0.331 (9)
N(1)	0.365 (8)	C(2)	0.153 (11)
N(2)	0.134 (7)		
(F) Plane VI through Ni, N(3), N(4), C(3), and C(4)			
$9.039x + 20.883y - 26.862z + 3.829 = 0$			
Ni	0.008 (7)	C(3)	-0.102 (13)
N(H)	0.415 (11)	C(4)	-0.015 (14)
N(3)	0.134 (9)		

Table X. Comparison of Average Bond Distances with Those from Other Neutron-Diffraction Studies of Amine Oxime Complexes of Ni(II)

	present compd	$[\text{Ni}(\text{EnAO-H})]\text{ClO}_4^a$	$[\text{Ni}(\text{AO})_2\text{-H}]^+\text{Cl}_2\text{H}_2\text{O}^b$
$\lambda_{\text{max}}(\text{H}_2\text{O}),^c$ nm	420, 268, 217	382, 263, 213	412, 265, 215
Ni-N(amine), Å	1.937 (5)	1.877 (2)	1.908 (2)
Ni-N(oxime), Å	1.884 (5)	1.841 (3)	1.866 (4)
N-O, Å	1.338 (7)	1.350 (2)	1.340 (5)
O...O, Å	2.409 (10)	2.478 (5)	2.420 (3)

^a Reference 4. ^b Reference 2. ^c Reference 13.

in agreement with the earlier observations pointing toward similarity of the steric requirements of PnAO and two coordinated AO's. The two chemically equivalent N-O distances and the N-N-O angles (Figure 5) agree extremely well, which is probably indicative of the highly symmetric nature of the intramolecular O-H...O bond. Amine oxime complexes having asymmetric intramolecular hydrogen bonds exhibit significantly unequal N-O distances and Ni-N-O angles within the same molecule.

The C-H distances range from 1.00 (2) to 1.12 (3) Å before the thermal motion corrections. The greatest thermal motion was found for the methyl groups attached to sp^2 carbon atoms. These show an average uncorrected C-H distance of 1.037 Å. After thermal motion correction (see thermal motion analysis), the average C-H distance for the methyl groups attached to sp^2 carbons increases to 1.114 Å while the average for those attached to sp^3 carbons is 1.102 Å, which is very close to the typical aliphatic distance of 1.09 Å. The average H-C-H angle (108°) is very close to the tetrahedral angle. The average N-H distance is 1.039 Å, and the average O-H distance is 0.92 Å. The average H-N-C angle is about 105° .

Intramolecular Hydrogen Bond. One of the objectives of this study was to compare the short hydrogen bond in this

Table XI. Asymmetry of Short O···O Hydrogen Bonds in α -Amine Oxime Complexes Studied by Neutron Diffraction (Distances in Å)

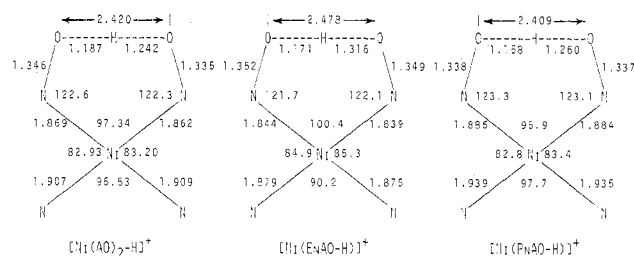
compd	O···O	O-H	O···H	$\Delta(O-H)$	ref
[Ni(AO) ₂ -H]Cl·H ₂ O	2.420 (3)	1.187 (5)	1.242 (5)	0.055 (10)	2
[Ni(EnAO-H)]ClO ₄	2.478 (5)	1.171 (8)	1.316 (8)	0.145 (16)	4
[Pt(AO) ₂ -H]Cl·3.5H ₂ O	2.472 (5)	1.087 (7)	1.389 (7)	0.302 (14)	3
[Ni(PnAO-H)]Cl·H ₂ O	2.409 (10)	1.158 (16)	1.260 (20)	0.102 (36)	this work

Table XII. Bond Summation and Bond Lengths (Å) Applied to the Short Hydrogen Bonds in Amine Oxime Complexes

compd	$S_t[O(1)]$	$S_t[O(2)]$	$S_t(H)$	distance		bond strength		O-H···O		ref
				O(1)-H	O(2)-H	O1-H	O2-H	predicted ^a	obsd	
[Ni(AO) ₂ -H]Cl·H ₂ O	2.089	2.031	0.947	1.187	1.242	0.497	0.450	2.45	2.42	2
[Pt(AO) ₂ -H]Cl·3.5H ₂ O	2.039	2.015	0.955	1.087	1.389	0.603	0.352	2.48	2.47	3
[Ni(EnAO-H)]ClO ₄	2.138	2.021	0.904	1.171	1.322	0.510	0.390	2.49	2.478	4
[Ni(PnAO-H)]Cl·H ₂ O	2.241	2.286	0.961	1.158	1.260	0.530	0.440	2.40	2.409	this work

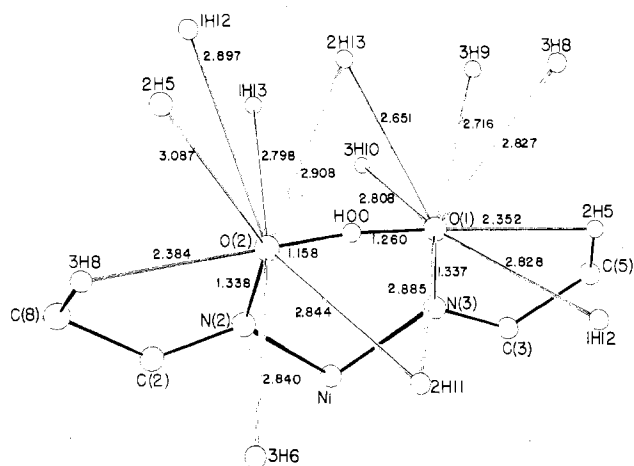
$$S_t = \Sigma S_i; S_i(O-H) = 0.50(R_i/1.184)^{-2.2}; S_i(O-N) = 1.667(R_i/1.241)^{-4.0}; R_i = \text{observed distance}$$

^a Calculated by using universal bond length-bond strength curves of Brown and Shannon.¹⁶

**Figure 4.** Variation of bond distances and the interchelate angles as a function of the steric requirements of the ligands.

complex with that in similar complexes. In Table XI the geometry of this hydrogen bond is compared with that found in other α -amine oxime complexes studied by neutron diffraction. A more extensive table comparing short hydrogen bonds is given by Fair and Schlemper.⁴ The O···O distance of 2.409 (10) Å observed in the present study is close to the shortest O···O distance 2.403 (3) Å observed by neutron diffraction analysis in $K[C_4H_2ClO_4]^-$,¹⁴ whereas it is 0.10 Å longer than 2.31 (1) Å, the shortest ever reported O···O distance observed in X-ray diffraction studies of Cu(II) and Ni(II) compounds of a diimine Schiff base.¹⁵ The O···O distance observed in the present work is within one standard deviation of that of 2.420 (3) Å observed in the case of [Ni(AO)₂-H]Cl·H₂O. The O···O distance observed in the X-ray study is 2.422 (6) Å which compares even better with 2.420 (3) Å observed in the [Ni(AO)₂-H]⁺ complex. The difference of 0.102 Å in O-H distances is within one standard deviation of that of 0.055 Å observed in [Ni(AO)₂-H]⁺ and is smaller than that of 0.145 Å observed in the case of [Ni(EnAO-H)]⁺, suggesting that the hydrogen bond may be as symmetrical in the present compound as in the case of [Ni(AO)₂-H]⁺.² The comparisons are somewhat limited by the high standard deviations in this study which result from the unavoidably poor neutron data to parameter ratio in the least-squares refinement. The interchelate ring angles shown in Figure 4 are also similar to those of [Ni(AO)₂-H]⁺ and are significantly different from those of [Ni(EnAO-H)]⁺, confirming our earlier conclusions that steric requirements of PnAO are nearly identical with two coordinated AO's and that a propylene bridge opposite the hydrogen bond has no significant influence on the hydrogen bond. The interchelate angles in [Ni(EnAO-H)]⁺ are significantly different from either the Ni-AO or Ni-PnAO complexes and so is the O···O distance which is ~ 0.05 Å longer for the EnAO complex. These dissimilarities are indicative of the strains imposed on the coordination geometry by the ethylene bridge in the EnAO ligand.

Using the approach suggested by Brown and Shannon,¹⁶ we compare the bonding for the O and H atoms of the short

**Figure 5.** The environments of the oxygen atoms involved in the short hydrogen bond. The standard deviations in the distances are O-H = 0.007–0.020.

hydrogen bonds in the α -amine oxime complexes studied by neutron diffraction in Table XII. When all O-H contacts less than 3.00 Å (Figure 5) were used to obtain the bond summation, the values of S_t are 2.241 and 2.286 for O(1) and O(2) atoms, respectively, rather than an ideal value ≈ 2.0 expected for these atoms. The higher S_t values suggest that longer intermolecular contacts are probably given too much weight in this treatment. Bond summation for the O atoms considering atoms within 2.4 Å gave S_t values of 1.781 for O(1) and 1.851 for O(2) atoms. The limiting distance of 2.4 Å includes only one intramolecular methyl hydrogen atom, contributing about 0.11 to S_t for each oxygen atom, similar to that for the AO- and EnAO-Ni(II) complexes.^{2,4} Similar calculations of the bond strength of the hydrogen atom in the hydrogen bond gave an S_t value of 0.961 compared to the expected value of about 1.0. Estimates of O-H distances based on predicted bond strengths and using universal bond strength-bond length curves of Brown and Shannon¹⁶ gave values for the O-H···O distances in very good agreement with the observed distances (Table XII).

The rigid-body thermal parameters¹⁷ (see next section) were subtracted from the thermal parameters for the individual atoms in the O-H···O bridge. For the analysis neglecting the screw motion, the root-mean-square amplitude of the difference ellipsoid of the hydrogen atom is 0.026 with an estimated standard deviation of 0.006 along the hydrogen bond axis. The average value in the two directions perpendicular to the O-H···O axis is close to zero. The thermal anisotropy of the hydrogen of the intramolecular hydrogen bond in the present study is in harmony with the short hydrogen bond in

Table XIII. Thermal Motion Analysis for the Methyl Groups of the Cation

methyl carbon ^a	U'_{11}	U'_{22} ^b	U'_{33}	r_{C-H} , Å	$\langle\theta\rangle$, deg	$r_{C-H}/\cos\langle\theta\rangle$	ω , ^d cm ⁻¹	V_0 , ^a kcal/mol
C(5) ^c	5 (3)	144 (70)	46 (32)	1.043 (26)	19.99	1.110	121	0.911
C(6)	9 (2)	43 (32)	11 (13)	1.087 (25)	10.79	1.108	222	3.049
C(7)	13 (6)	39 (5)	21 (7)	1.077 (19)	10.39	1.095	233	3.362
C(8) ^c	13 (12)	189 (43)	38 (42)	1.031 (33)	22.9	1.119	105	0.694
C(9)	8 (7)	64 (18)	16 (12)	1.083 (44)	13.2	1.112	181	2.049
C(10)	27 (9)	53 (20)	13 (15)	1.067 (25)	12.2	1.091	203	2.474

^a The U' are mean-square amplitudes $U_{\text{exptl}} - U_{\text{rigid body}} (\times 10^3) \text{ \AA}^2$. r_{C-H} is the uncorrected bond length, θ is the root-mean-square amplitude of rotation calculated by $\tan\langle\theta\rangle = (U_{22})^{1/2}/r_{C-H}$, V_0 is the barrier height obtained from $V_0 = 0.0040T/U'_{22}n^2$ where $T = 295 \text{ K}$ (i.e., approximate room temperature). ^b The natural axes are defined so that U'_{22} is the hindered rotation, i.e., axis 1 is along the C-C bond, axis 3 is in the C-C-H plane, and axis 2 completes the orthogonal system. ^c Methyl carbon atoms attached to sp^2 carbon atoms. ^d ω (cm⁻¹) = $76.8n(V_0/\text{kcal/mol})/I(\text{amu \AA}^2)^{1/2}$ where $n = 3$, moment of inertia $I = \sum m_i r_i^2$; $m_H = 1.008 \text{ amu}$, $r = r_{C-H}$ (corrected) $\times \cos 19.5^\circ$. For more details, see ref 2.

Chart I

$$T(\text{\AA}^2) = \begin{pmatrix} 0.034 (1) & -0.001 (1) & 0.005 (1) \\ -0.001 (1) & 0.300 (2) & 0.003 (2) \\ 0.005 (1) & 0.003 (2) & 0.024 (2) \end{pmatrix}$$

$$L(\text{deg}^2) = \begin{pmatrix} 14.8 (15) & -3.3 (7) & 5.1 (5) \\ -3.3 (7) & 12.2 (8) & 0.5 (6) \\ 5.1 (5) & 0.5 (6) & 8.7 (7) \end{pmatrix}$$

$$S(\text{deg \AA}) = \begin{pmatrix} 0.02 (4) & -0.03 (3) & 0.05 (3) \\ 0.04 (2) & 0.02 (3) & -0.04 (2) \\ 0.01 (2) & -0.05 (3) & 0.04 (32) \end{pmatrix}$$

the $[\text{Ni}(\text{AO})_2\text{-H}]^{+2}$ or in potassium hydrogen diaspinate¹⁸ and in marked contrast to the distinctly different thermal anisotropy observed for the $[\text{Pt}(\text{AO})_2\text{-H}]^+$ complex.³ The elongation along the O—H...O direction suggests a broad single-minimum potential with appreciable static disorder. The difference nuclear thermal ellipsoids for the O atoms are very small with an average root-mean-square value of 0.004 (3) Å.

Analysis of Thermal Motion The root-mean-square components of thermal motion along principal axes for all atoms are available,¹² and the directions of vibration can be seen in Figure 3. For most of the nonhydrogen atoms, the minimum and maximum amplitudes vary by less than a factor of 2. The methyl group hydrogen atoms have larger amplitudes of vibration which led to a treatment¹⁷ of thermal motion in which the terminal methyl groups are treated as hindered rotors.

The thermal motion parameters of the 20 nonhydrogen atoms in the positive ion were fitted to a general rigid-body model of 21 parameters as described by Schomaker and Trueblood.¹⁷ The anisotropic β_{ij} were converted to mean-square amplitudes U_{ij} and referred to an orthogonal axial system with the first axis parallel to the crystal a , the second to $c^* \times a$, and the third to the c^* axes. The translation tensor (T), libration tensor (L), and interaction tensor (S), referred to the same axis system, are given in Chart I.

The root-mean-square length along the principal axes of libration and translation are $L = 4.34, 3.42$, and 2.27° and $T = 0.19, 0.18$, and 0.15 \AA . The principal libration and translation axes are nearly coincident. The root-mean-square translational amplitudes are almost identical with those of the $[\text{Ni}(\text{AO})_2\text{-H}]\text{Cl}\cdot\text{H}_2\text{O}$ complex² and slightly larger than those for $[\text{Pt}(\text{AO})_2\text{-H}]\text{Cl}\cdot 3.5\text{H}_2\text{O}$.³ The largest librational and translational amplitudes are around and in the direction of the long axis of the molecule, as observed in the Ni- and Pt-AO complexes.^{2,3}

The screw components are small and similar to those in the case of $[\text{Ni}(\text{AO})_2\text{H}]\text{Cl}\cdot\text{H}_2\text{O}$ and smaller than in the Pt-AO complex. The effective translations in the nonintersecting axis description are 0.009, -0.007, and -0.007 Å. The root-mean-square deviation of the experimental U_{ij} from those calculated from the least-squares values of T , L , and S is 0.0055 Å. This suggests significant nonrigid-body motion in

the complex. The "center of reaction" is very similar to the center of the mass of the heavy atoms, lying within 0.01 Å of each other. Because of the small size of the screw components, an analysis in terms of T and L was chosen. The root-mean-square deviation of U_{ij} in that analysis was 0.0061 Å² and the root-mean-square lengths and direction of the principal axes of T and L show little change: $L = 4.46, 3.44, 2.28$; $T = 0.19, 0.18, 0.14$. The center of mass of the 20 nonhydrogen atoms was taken as the origin for the libration axes.

The amplitude of vibration of the methyl H atoms was corrected for the rigid-body motion obtained above for the $S = 0$ case. The resulting ΔU 's ($U_{\text{exptl}} - U_{\text{rigid body}}$) were analyzed in terms of hindered rotation as in the case of the Ni(II)- and Pt(II)-AO complexes to derive root-mean-square amplitudes of hindered rotation (θ), estimated vibrational frequencies (ω), and corresponding barrier heights (V_0) (Table XIII). In almost every case, the largest amplitude of the difference ellipsoid was in the direction of axis 2 which corresponds to the hindered rotation of the methyl group.

From this analysis it can be seen that the methyl groups on the sp^2 C atoms, i.e., C(5) and C(8) methyl groups, have larger amplitudes and lower frequencies than the methyl groups on the sp^3 C atoms. The barrier heights, V_0 , for the C(5) and C(8) methyl groups are therefore significantly smaller than that for other methyl groups. The agreement between the corrected bond distances is excellent. The results of thermal analysis are in good agreement with similar analyses for the Ni(II)- and Pt(II)-AO complexes.^{2,3}

Acknowledgment. Financial support from the National Science Foundation (Grant CHE 77-08325) is gratefully acknowledged. We are thankful to Professor R. K. Murmann for communicating results of the spectral and thermodynamic studies of these complexes prior to publication.

Registry No. $[\text{Ni}(\text{PnAO-H})]\text{Cl}\cdot\text{H}_2\text{O}$, 70369-10-7; $[\text{Ni}(\text{PnAO-H})]\text{Cl}\cdot 1.5\text{H}_2\text{O}$, 70368-93-3.

Supplementary Material Available: Table V, anisotropic thermal parameters of nonhydrogen atoms in $[\text{Ni}(\text{PnAO-H})]\text{Cl}\cdot\text{H}_2\text{O}$ from neutron diffraction data, Table VI, anisotropic thermal parameters for nonhydrogen atoms in $[\text{Ni}(\text{PnAO-H})]\text{Cl}\cdot\text{H}_2\text{O}$ from X-ray diffraction data, Table VII, anisotropic thermal parameters for hydrogen atoms in $[\text{Ni}(\text{PnAO-H})]\text{Cl}\cdot\text{H}_2\text{O}$ for neutron diffraction data, Table XIV, root-mean-square components (Å) of thermal displacement along the principal axes of the ellipsoids, Table XV, observed and calculated structure factors ($\times 10$) for neutron diffraction data, and Table XVI, observed and calculated structure factors ($\times 10$) for X-ray diffraction data (31 pages). Ordering information is given on any current masthead page.

References and Notes

- Hussain, M. S.; Salinas, B. E. V.; Schlemper, E. O. *Acta Crystallogr., Sect. B* **1979**, *35*, 628.
- Schlemper, E. O.; Hamilton, W. C.; LaPlaca, S. J. *J. Chem. Phys.* **1971**, *54*, 3990.
- Schlemper, E. O.; Fair, C. K. *Acta Crystallogr., Sect. B* **1977**, *33*, 2482.

- (4) Fair, C. K.; Schlemper, E. O. *Acta Crystallogr., Sect. B* **1978**, *34*, 436.
 (5) Hussain, M. S.; Schlemper, E. O. *Inorg. Chem.* **1979**, *18*, 1116, and references therein.
 (6) Vassian, E. G.; Murmann, R. K. *Inorg. Chem.* **1967**, *6*, 2043.
 (7) Cameron, T. S.; Mannan, Kh. M.; Rehman, Md. O. *Acta Crystallogr., Sect. B* **1976**, *32*, 87.
 (8) (a) Stewart, R. F.; Davidson, E. R.; Simpson, W. T. *J. Chem. Phys.* **1965**, *42*, 3175. (b) Cromer, D. T.; Waber, J. T. *Acta Crystallogr.*, **1962**, *18*, 104. (c) Cromer, D. T. *Ibid.* **1962**, *18*, 17. (d) Ibers, J. A.; Hamilton, W. C. *Ibid.* **1964**, *19*, 781. (e) "International Tables for X-Ray Crystallography"; Kynoch Press: Birmingham, England; Vol. IV, p 270, Tables 2-6.
 (9) All calculations were performed on the University of Missouri IBM 370/168 computer systems by using the following programs: ANGSET, angle settings program; SORTH, W. C. Hamilton's sorting program; HORSE, W. C. Hamilton's general absorption correction program; ORFE, function and error program; H FIND, A. Zalkin's hydrogen position calculation program; FAME, normalized structure factor calculation program; MULTAN, P. Main's, Woolfson's, and G. Germain's programs for automatic solution of crystal structure; ORTEP, C. Johnson's thermal ellipsoid plot program.
 (10) $R(F_o^2) = \sum |F_o^2 - KF_c^2| / \sum F_o^2$ and $R_w(F^2) = [\sum w(F_o^2 - kF_c^2)^2 / \sum wF_o^4]^{1/2}$. All least-squares refinements were based on the minimization of $\sum w(F_o^2 - F_c^2)^2$ with individual weights $w = 1/\sigma^2(F_o^2)$.
 (11) Peerdeman, A. F.; Bijoet *Acta Crystallogr.* **1956**, *9*, 1012.
 (12) Supplementary material.
 (13) Murmann, R. K., private communication, to be submitted for publication.
 (14) Ellison, R. D.; Levy, H. A. *Acta Crystallogr.* **1965**, *19*, 260.
 (15) Bertrand, J. A.; Black, T. D.; Eller, P. G.; Helm, F. T.; Mahmood, R. *Inorg. Chem.* **1976**, *15*, 2965.
 (16) Brown, I. D.; Shannon *Acta Crystallogr., Sect. A* **1973**, *29*, 266.
 (17) Schomaker, V.; Trueblood, K. W. *Acta Crystallogr., Sect. B* **1968**, *24*, 63.
 (18) Sequiera, A.; Berkebile, C. A.; Hamilton, W. C. *J. Mol. Struct.* **1967**, *1*, 283.

Contribution from the Istituto di Chimica Generale, Università di Pisa, 56100 Pisa, Italy, and the Centro di Studio per la Strutturistica Diffraattometrica del CNR, Istituto di Strutturistica Chimica, Università di Parma, 43100 Parma, Italy

Vanadium-Olefin and -Acetylene Complexes: Structural Studies on (η^2 -Diethyl fumarato-*C,C*)- and (η^2 -Dimethyl acetylenedicarboxylato-*C,C*)bis(η -cyclopentadienyl)vanadium

GIUSEPPE FACHINETTI, CARLO FLORIANI,* ANGIOLA CHIESI-VILLA, and CARLO GUASTINI

Received March 16, 1979

Vanadocene, $(\text{cp})_2\text{V}$ ($\text{cp} = \eta^5\text{-C}_5\text{H}_5$), adds as a carbene-like species to the $\text{C}=\text{C}$ bond of diethyl fumarate or diethyl maleate, producing the same monomeric olefinic complex (IV) in which the coordinated olefin assumes the trans configuration. Diethyl maleate isomerizes upon coordination to the metal. Vanadium is η^2 bonded to the two Cp rings, which are in a bent arrangement making a cavity in the equatorial plane for the $\eta^2\text{-C,C}$ bonded olefinic ligand [$\text{cp}(1)\text{-V-cp}(2) = 135.9^\circ$]. The $\text{C}=\text{C}$ bond distance is significantly lengthened by interaction with the metal to the value [1.468 (11) Å] expected for a single bond. Vanadocene reacts with $\text{CH}_3\text{O}_2\text{C}-\text{C}\equiv\text{C}-\text{CO}_2\text{CH}_3$ giving complex V with an overall geometry very similar to that found for the olefinic complex. The coordinated $\text{C}-\text{C}$ bond length [1.287 (4) Å] is nearly close to that of a double bond. Both complexes have rigorous C_2 symmetry. They represent rare examples of vanadocene with an additional $\text{V}-\text{C}$ bond for which structural data are available [$\text{V}-\text{C} = 2.186$ (12) and 2.213 (12) Å for $(\text{cp})_2\text{V}(\text{C}_2\text{H}_5\text{O}_2\text{CCH}-\text{CHCO}_2\text{C}_2\text{H}_5)$ and 2.097 (3) and 2.084 (3) Å for $(\text{cp})_2\text{V}(\text{CH}_3\text{O}_2\text{CC}=\text{CCO}_2\text{CH}_3)$]. Crystallographic details for $(\text{cp})_2\text{V}(\text{C}_2\text{H}_5\text{O}_2\text{C}-\text{CH}-\text{CH}-\text{CO}_2\text{C}_2\text{H}_5)$: space group $P2_1/c$ (monoclinic); $a = 7.871$ (1), $b = 18.604$ (3), $c = 13.712$ (3) Å; $\beta = 121.32$ (2)°; $U = 1715.3$ Å³; $Z = 4$; $D_c = 1.368$ g cm⁻³. The final R factor was 6.5% for 2321 observed reflections. Crystallographic details for $(\text{cp})_2\text{V}(\text{CH}_3\text{O}_2\text{C}-\text{C}\equiv\text{C}-\text{CO}_2\text{CH}_3)$: space group C_2/c (monoclinic); $a = 25.089$ (2), $b = 7.948$ (1), $c = 15.979$ (2) Å; $\beta = 112.14$ (1)°; $U = 2951.4$ Å³; $Z = 8$; $D_c = 1.455$ g cm⁻³. The final R factor was 4.4% for 2408 observed reflections.

Introduction

While the olefin and acetylene metal-promoted reactivity is very well-known in titanium and vanadium bis(cyclopentadienyl) chemistry,¹ structural evidence on acetylene and olefin complexes is practically absent. Only very recently we described the first diphenylacetylene $\eta^2\text{-C,C}$ bonded to titanium in $(\text{cp})_2\text{Ti}(\text{CO})(\text{Ph}_2\text{C}_2)$ ($\text{cp} = \eta^5\text{-C}_5\text{H}_5$).² The interest in π olefin and π acetylene complexes of titanium and vanadium stems from the special activity of these metals which are able to promote polymerization, oligomerization, and catalytic hydrogenation of these unsaturated substrates.¹⁻³ This notwithstanding, we did not find structural models for vanadium-olefin⁴ and vanadium-acetylene interaction.^{3,5} Moreover, structural data on vanadocenes bearing an additional vanadium-carbon bond are limited to only the few cases reported in Table VIII.^{6,7} As a part of our continuing investigations into the structure and chemical properties of bis(cyclopentadienyl) derivatives of early transition metals, we report here the structural properties of $(\text{cp})_2\text{V}(\text{EtO}_2\text{CCH}-\text{CHCO}_2\text{Et})$ ⁴ and $(\text{cp})_2\text{V}(\text{MeO}_2\text{CC}=\text{CCO}_2\text{Me})$.³

* To whom correspondence should be addressed at the Università di Pisa.

Experimental Section

Sample Preparations. The direct synthesis gave diffraction-quality crystals. Both complexes are reasonably air-stable in the solid state. Complex IV, $(\text{cp})_2\text{V}(\text{EtO}_2\text{CCH}-\text{CHCO}_2\text{Et})$, was prepared from diethyl maleate.⁴ The slightly modified version used for the synthesis of complex V,³ $(\text{cp})_2\text{V}(\text{MeO}_2\text{CC}=\text{CCO}_2\text{Me})$, is given below.

Synthesis of $(\text{cp})_2\text{V}(\text{MeO}_2\text{CC}=\text{CCO}_2\text{Me})$. A benzene (20 mL) solution of $(\text{cp})_2\text{V}$ (0.85 g, 4.70 mmol) is reacted with neat $\text{MeO}_2\text{CC}=\text{CCO}_2\text{Me}$ (0.72 mL, 5.1 mmol). The solution color turns suddenly to deep green. Green crystals suitable for an X-ray analysis start to separate in 15 min. The yield of $(\text{cp})_2\text{V}(\text{MeO}_2\text{CC}=\text{CCO}_2\text{Me})$ is increased by adding heptane (50 mL) to the solution. The overall yield is ca. 70%. Anal. Calcd for $\text{C}_{16}\text{H}_{16}\text{O}_4\text{V}$: C, 59.44; H, 4.95. Found: C, 59.11; H, 5.10. The IR spectrum in Nujol shows a strong band at 1820 cm⁻¹ ($\nu_{\text{C}=\text{C}}$) and a strong band of complex envelope centered at 1670 cm⁻¹ ($\nu_{\text{C}=\text{O}}$).

X-ray Data Collection and Structure Refinement.⁸ The crystals examined were wedged into thin-walled glass capillaries which were sealed under nitrogen. They were mounted with the [001] axis along the Φ axis of the diffractometer. A summary of the crystal and intensity data collection is given in Table I. Lattice constants came from least-squares refinements of the 2θ values for 31 reflections [$2\theta > 40^\circ$ for IV, $2\theta > 100^\circ$ for V].